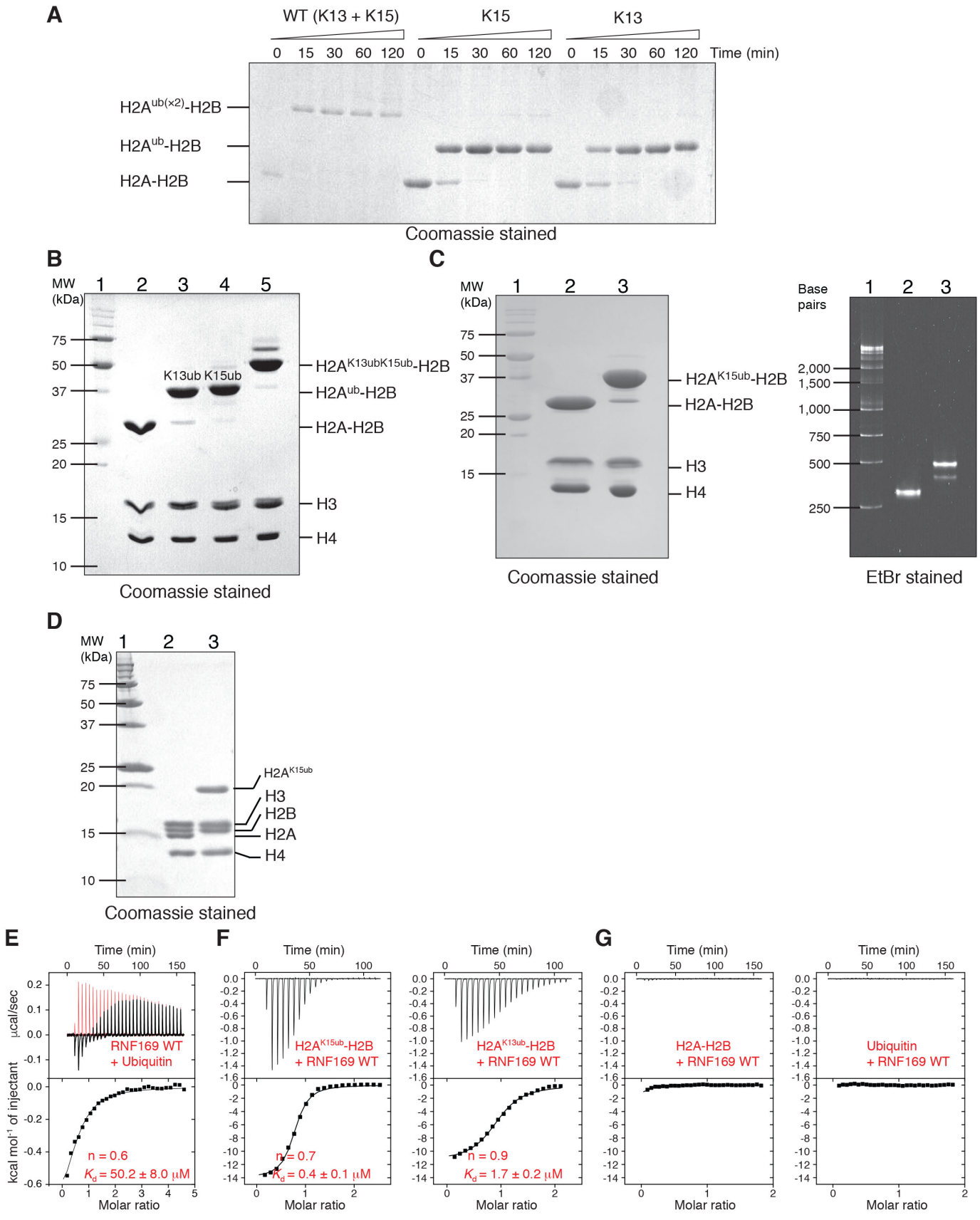


**Figure S1. Preparation of ubiquitylated H2A-H2B and NCP, Related to Figures 1, 2 and 3**
(A) Enzymatic ubiquitylation of wild type, K13S mutant and K15S mutant of H2A-H2B fusion (short version) by RNF168 highlighting high efficiency ubiquitylation at H2A Lys13 and Lys15, Lys15, and

Lys13, respectively. Aliquots of the reaction mixtures were taken at different time points and analyzed on an 18% SDS PAGE gel stained with Coomassie.
(B) Coomassie stained 18% SDS PAGE gel of the human NCP reconstituted with an octamer of H3, H4 and the long version of H2A-H2B fusion non-ubiquitylated (lane 2) and enzymatically mono-ubiquitylated by RNF168 at H2A Lys13 (lane 3), H2A Lys15 (lane 4), and di-mono-ubiquitylated at H2A Lys13 and Lys15 ($H2A^{K13ubK15ub}$-H2B) (lane 5).
(C) Left: Coomassie stained 18% SDS PAGE gel of the human NCP (lane 2) and $NCP^{K15ub}$ (lane 3) samples used for NMR studies. NCP is reconstituted with a 147 base-pair DNA with the Widom 601 sequence and an octamer composed of fully deuterated H3 and H4, and the long version of H2A-H2B that is deuterated and selectively [$^{1}$H, $^{13}$C]-labeled at the Ile, Leu and Val methyl groups. $NCP^{K15ub}$ is prepared similarly as NCP but using $H2A^{K15ub}$-H2B where the ubiquitin component is fully deuterated. Right: Corresponding 5% native PAGE gel of the human NCP (lane 2) and $NCP^{K15ub}$ (lane 3) stained with ethidium bromide.
(D) Coomassie stained 18% SDS PAGE gel of the human NCP (lane 2) and NCP with H2AK15 ubiquitylation mimic (lane 3) created by fusion of ubiquitin to the N-terminus of H2A as described in the Methods section.
(E) ITC results (top, raw titration data; bottom, integrated heat measurements) for the interaction of RNF169 with ubiquitin. Because of the weak binding, high concentrations of RNF169 (148 μM in calorimeter cell) and ubiquitin (3 mM in injection syringe) were used to derive an accurate $K_d$. The red signals correspond to the heat of dilution of ubiquitin in the buffer solution.
(F) ITC results for the interactions of RNF169 with $H2A^{K15ub}$-H2B and $H2A^{K13ub}$-H2B mimics in which the C-terminal Gly76 of ubiquitin is genetically linked to the N-terminus of H2A Thr16 or Ala14, respectively, via two intervening glycine residues. $H2A^{K15ub}$-H2B and $H2A^{K13ub}$-H2B were in the calorimeter cell and RNF169 was in the injection syringe. n is the stoichiometry of binding. $K_d$s are reported with s.d. determined by nonlinear least-squares analysis.
(G) ITC results for the interactions of RNF169 with H2A-H2B and ubiquitin highlighting weak binding.

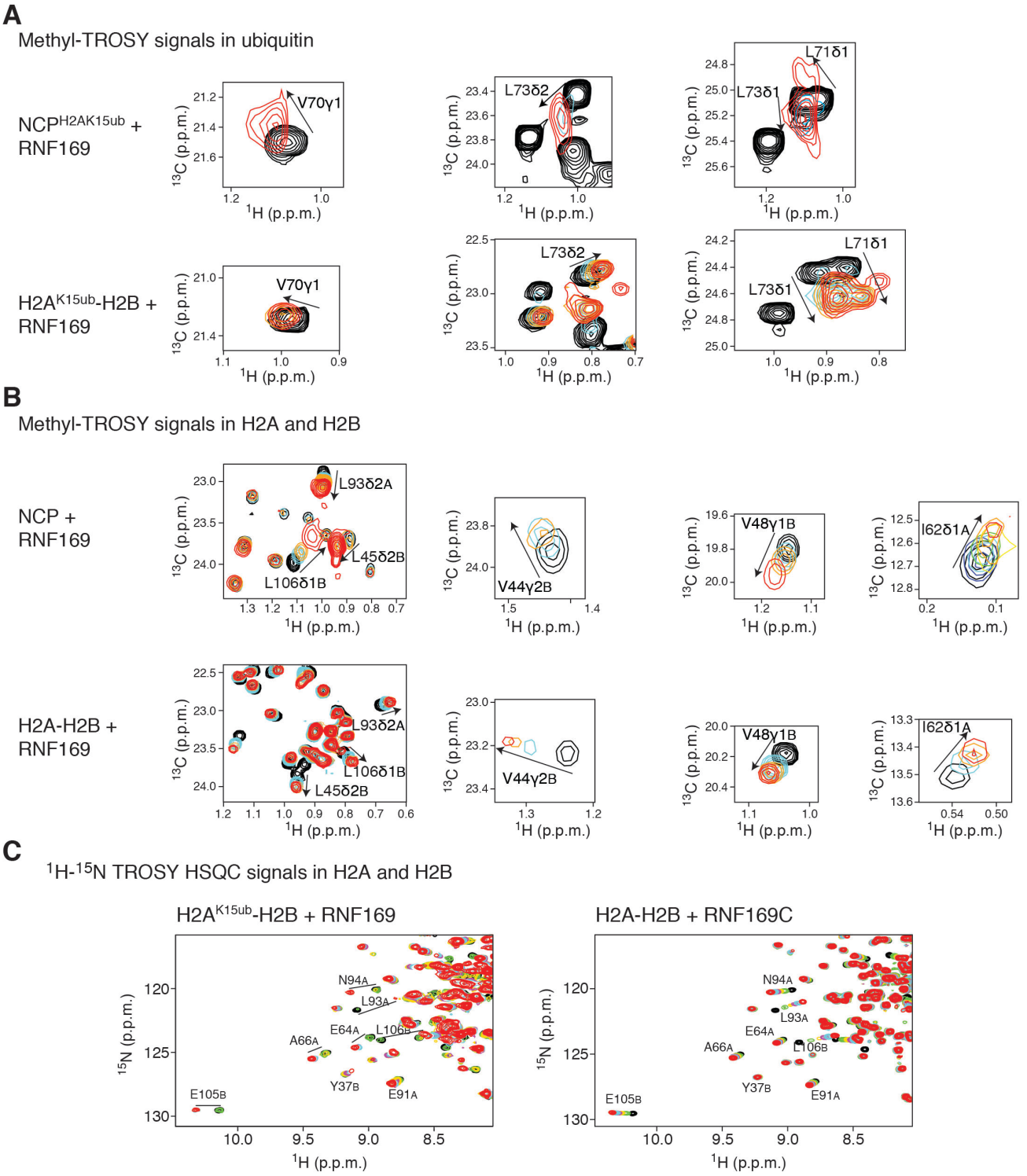


**Figure S2. Interaction of RNF169 with NCP, H2A-H2B, NCP$^{H2AK15ub}$ and H2A$^{K15ub}$-H2B probed by methyl-TROSY NMR and $^{1}$H-$^{15}$N TROSY HSQC, Related to Figures 2 and 3**

(A) Comparison of chemical shift perturbations in ubiquitin caused by RNF169 in the context of NCP$^{H2AK15ub}$ (top spectra) and H2A$^{K15ub}$-H2B (bottom spectra).

(B) Comparison of chemical shift perturbations in H2A and H2B caused by RNF169 in the context of NCP (top spectra) and H2A-H2B (bottom spectra).

(C) Comparison of chemical shift perturbations in H2A and H2B caused by RNF169 (aa 653-708) in the context of H2A$^{K15ub}$-H2B (left spectra) and by RNF169C (aa 688-704) in the context of H2A-H2B (right spectra). Notice the slow exchange on the chemical shift time scale in the left spectra and fast exchange in the right spectra.

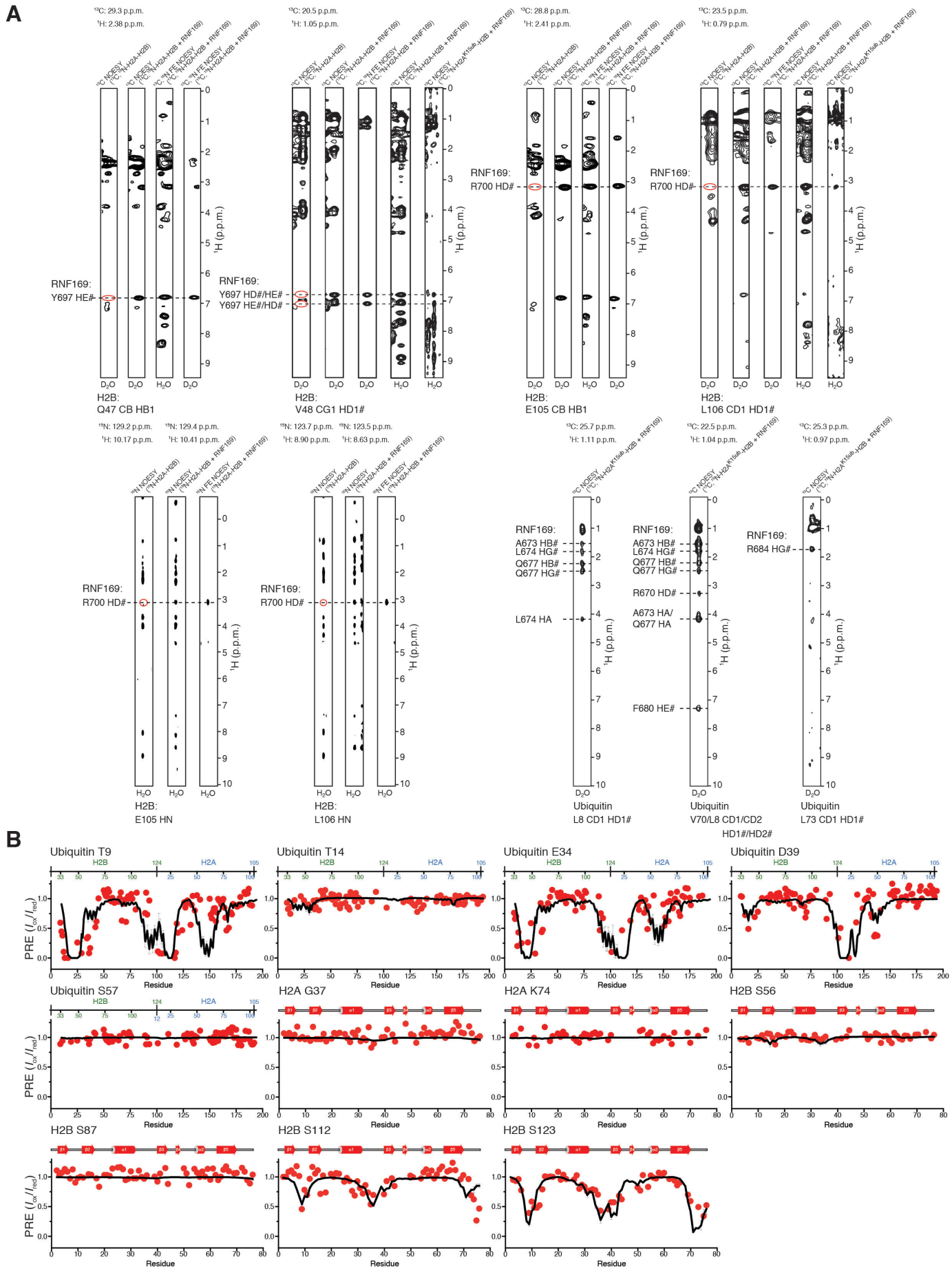


**Figure S3. Intermolecular NOEs and PREs defining the interaction of RNF169 with H2A$^{K15ub}$-H2B, Related to Figure 3**

(A) Selected regions of $^{13}C$-edited, $^{15}N$-edited and $^{13}C/^{15}N$-filtered-edited NOESY spectra of H2A-H2B, H2A-H2B–RNF169 and $H2A^{K15ub}$-H2B–RNF169 illustrating how intermolecular NOEs were identified and validated.
(B) Experimental (red disks) and back-calculated intermolecular PRE values (black lines with error bars indicating mean ± s.d.) for an ensemble of 20 NMR structures. MTSL spin labels were at indicated ubiquitin, H2A or H2B positions (see Methods).

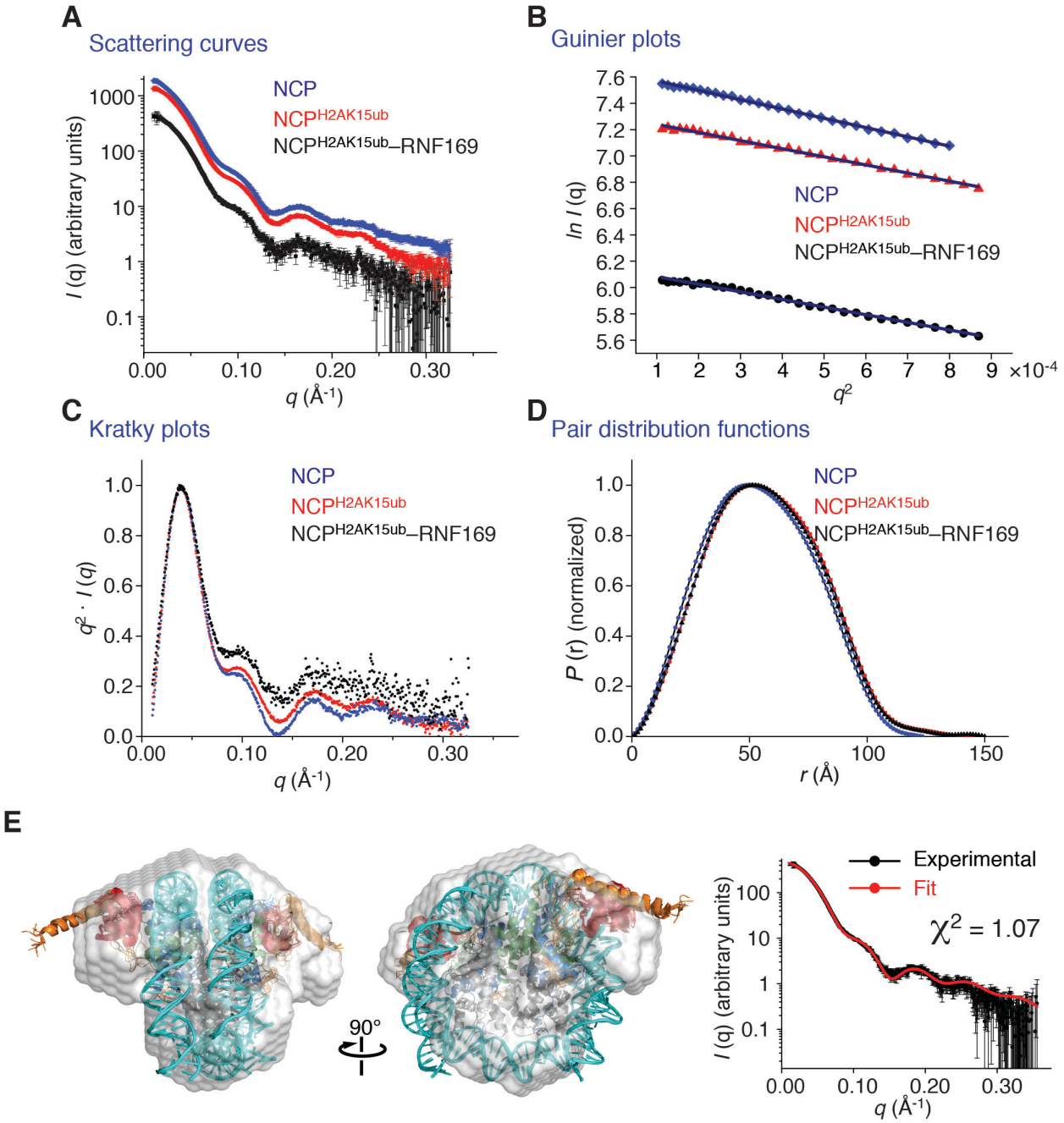


**Figure S4. Small-angle X-ray scattering (SAXS) of NCP, NCP$^{H2AK15ub}$ and NCP$^{H2AK15ub}$–RNF169, Related to Figure 3**

(A) Scattering curves $I(q)$ vs. $q$ where $q = 4\pi.\sin\theta/\lambda$.

(B) Guinier plots showing linearity at very low angle ($q.R_g < 1.3$) where $R_g$ is the radius of gyration.

(C) Normalized Kratky plots.

(D) Normalized pair distribution functions.

(E) Left: Cartoon representation of NCP $^{H2AK15ub}$–RNF169 NMR-derived model overlaid to the *ab initio* molecular envelope of NCP $^{H2AK15ub}$–RNF169 reconstructed using DAMMIF. Right: Scattering curve back-calculated from NCP$^{H2AK15ub}$–RNF169 NMR-derived model (red) overlaid to experimental SAXS data (black). Data were analyzed using CRYSOL. The normalized spatial discrepancy value is 0.648. Goodness of fit $\chi^2$ is indicated.

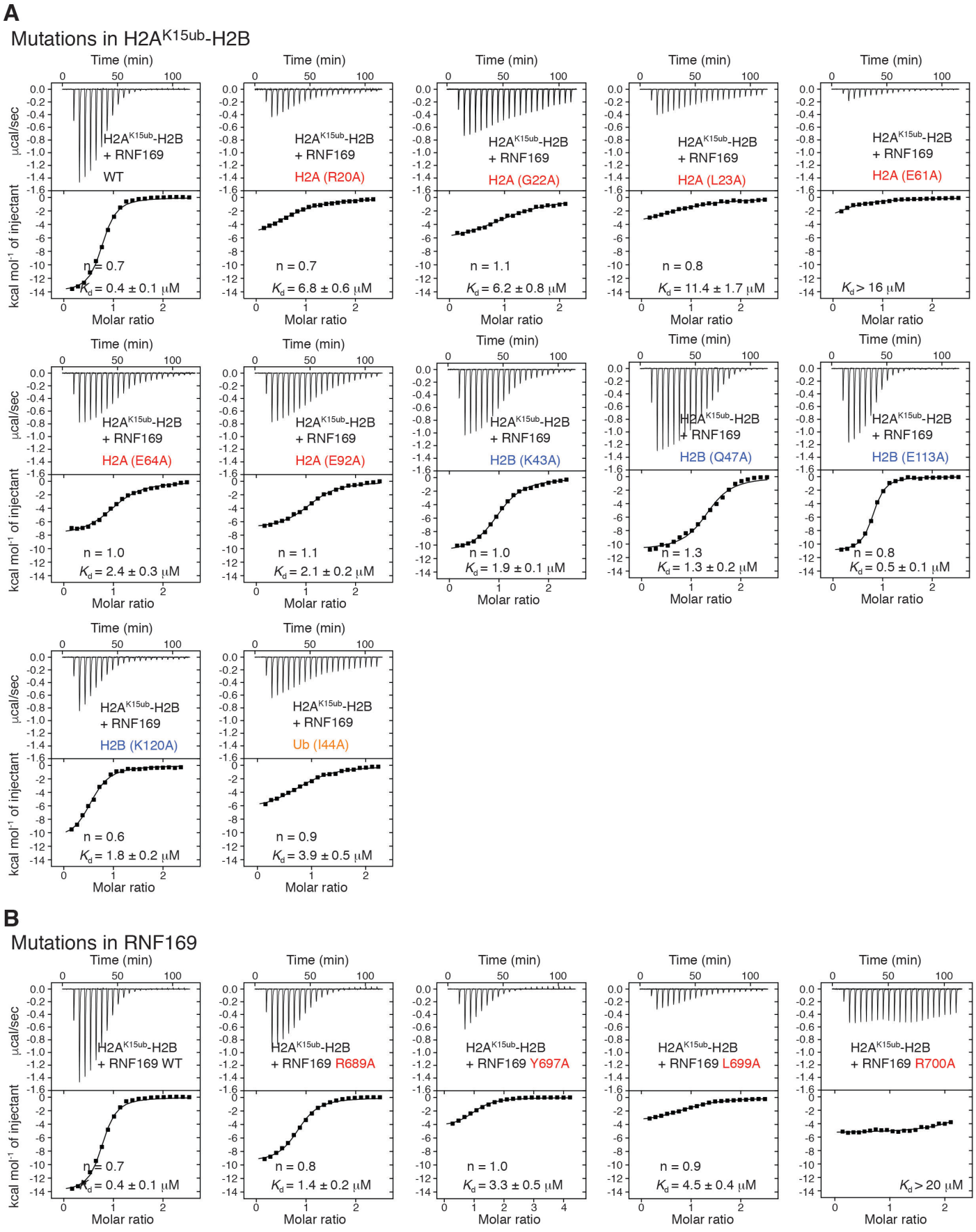


**Figure S5. Effects of mutations on the affinity of RNF169 for H2A$^{K15ub}$-H2B, Related to Figure 3**

(A) ITC results (top, raw titration data; bottom, integrated heat measurements) of the effect of mutations introduced in H2A, H2B or ubiquitin in $H2A^{K15ub}$-H2B on its interaction with wild type (WT) RNF169. The titration of WT $H2A^{K15ub}$-H2B with WT RNF169 is shown on the left for reference. $H2A^{K15ub}$-H2B was in the calorimeter cell and RNF169 was in the injection syringe. n is the stoichiometry of binding. $K_d$s are reported with s.d. determined by nonlinear least-squares analysis. All experiments were done under identical conditions and scaled in the same way to emphasize the effect of mutations on binding.
(B) ITC results of the effect of mutations introduced in RNF169 on the interaction with wild type (WT) $H2A^{K15ub}$-H2B. The titration of WT $H2A^{K15ub}$-H2B with WT RNF169 is shown on the left for reference. $H2A^{K15ub}$-H2B was in the calorimeter cell and RNF169 was in the injection syringe.

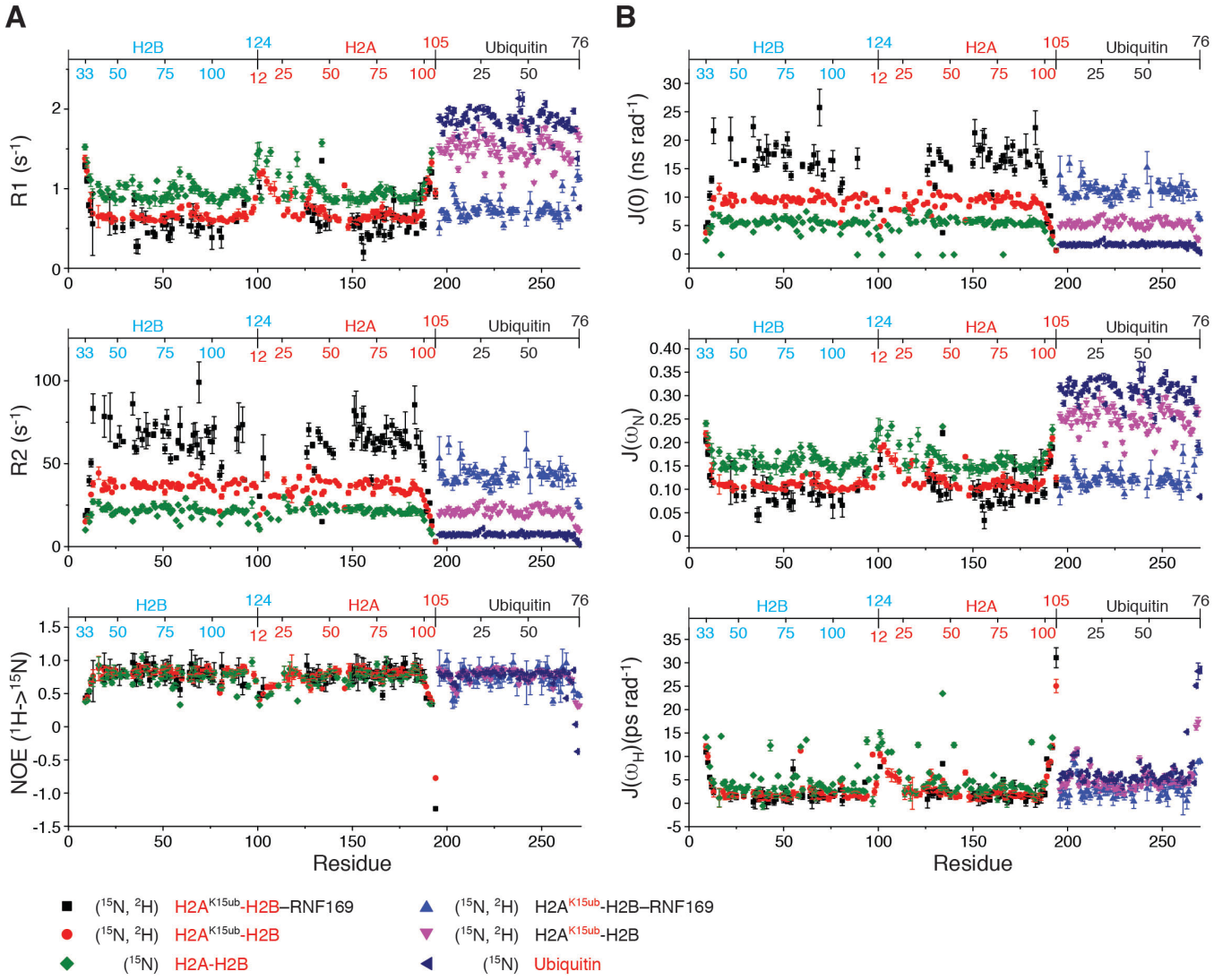


**Figure S6. NMR relaxation measurements, Related to Figures 3, 4 and 5**

(A) Backbone $^{15}$N-spin relaxation parameters R1, R2 and $^{15}$N-($^{1}$H) steady-state nuclear Overhauser effect (NOE) for H2A and H2B in H2A-H2B, H2A$^{K15ub}$-H2B and H2A$^{K15ub}$-H2B–RNF169 complex; and for ubiquitin, free and in H2A$^{K15ub}$-H2B and H2A$^{K15ub}$-H2B–RNF169 complex.

(B) Reduced spectral density functions J(0), J($\omega_N$) and J($\omega_H$) calculated using the relaxation data in Figure S6A.

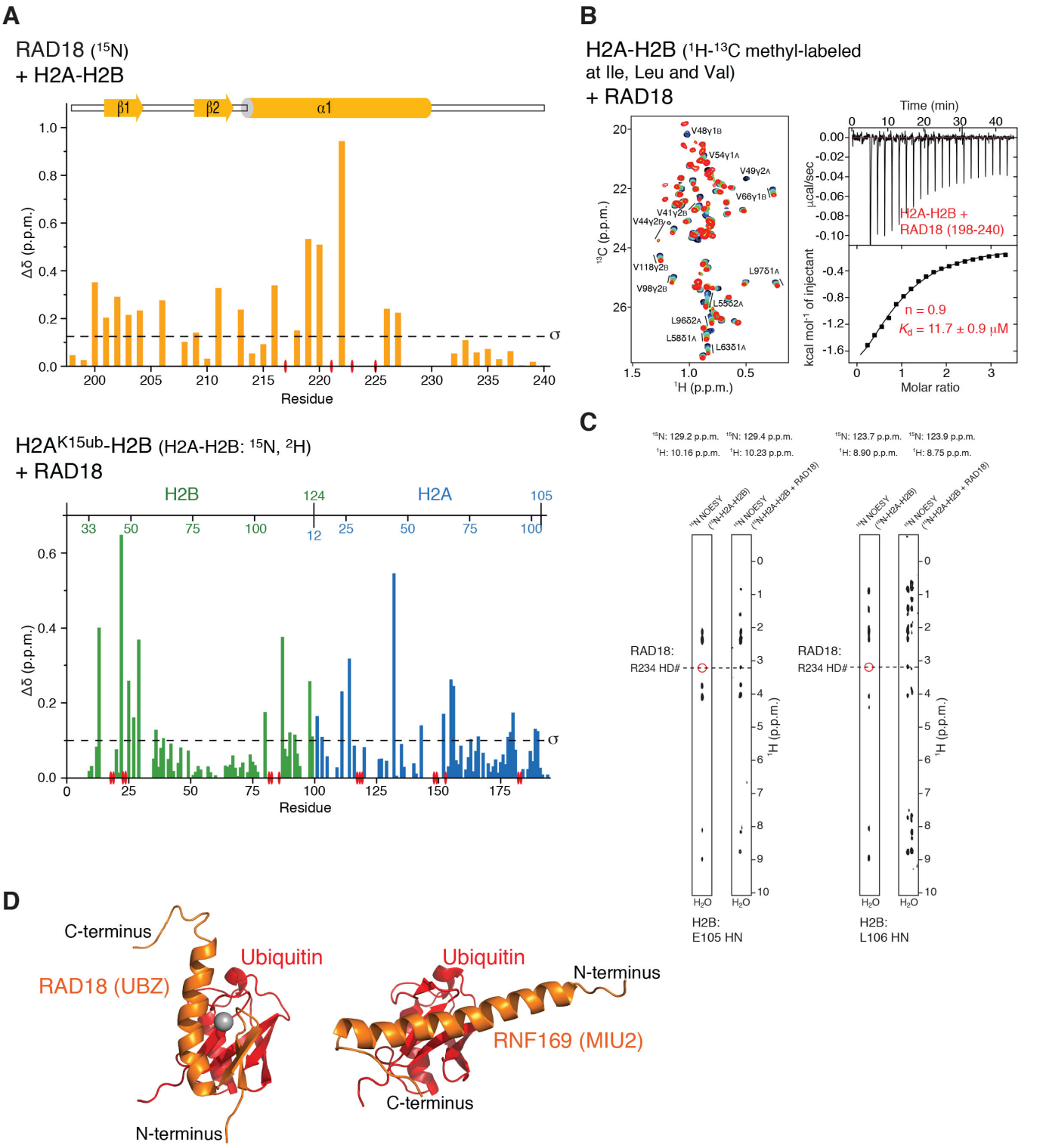


**Figure S7. NMR characterization of RAD18 interaction with H2A-H2B and H2A$^{K15ub}$-H2B, Related to Figure 7**

(A) Top: Magnitude of $^{1}$H-$^{15}$N chemical shift changes in RAD18 (aa 198-240) in the context of H2A$^{K15ub}$-H2B after addition of 3.5-fold molar excess H2A-H2B. Residues for which signals disappear due to exchange broadening are indicated with red elliptical disks on the x axis. Corresponding titration spectra are in Figure 7B top left. Bottom: Magnitude of $^{1}$H-$^{15}$N chemical shift changes in H2A (blue) and H2B (green) in the context of H2A$^{K15ub}$-H2B after addition of 5-fold molar excess RAD18 (aa 198-240). Corresponding titration spectra are in Figure 7B bottom left.

(B) Left: Region of methyl-TROSY spectra of H2A-H2B selectively $^{1}H$-$^{13}C$ methyl labeled at Ile, Leu and Val in a perdeuterated background (black) and in the presence of increasing amounts of unlabeled RAD18 (aa 198-240). Right: The $K_d$ for the H2A-H2B–RAD18 (aa 198-240) interaction was estimated using ITC.
(C) Selected regions of $^{15}N$-edited NOESY spectra of $^{15}N$-labeled/30% deuterated H2A-H2B, free, and H2A-H2B in presence of ~100-fold molar excess unlabeled RAD18 (aa 227-238), showing that intermolecular NOEs are detected between RAD18 Arg234 and H2B Glu105 and Leu106.
(D) Comparison of ubiquitin–RAD18 UBZ and ubiquitin–RNF169 MIU2 interactions illustrating the two radically different binding modes. The zinc atom is shown as a gray sphere.

**Table S1. Experiments used for NMR resonance assignments and identification of NOEs for structure determination of H2A$^{K15ub}$-H2B–RNF169, Related to Figures 2 and 3**

| | Purpose | NMR experiment | Sample |
|---|---|---|---|
| H2A-H2B | Backbone assignments | TRHNCO | 100% $^{2}$H, $^{13}$C, $^{15}$N H2A-H2B |
| | | TRHNCOCACB | 100% $^{2}$H, $^{13}$C, $^{15}$N H2A-H2B |
| | | TRHNCACB | 100% $^{2}$H, $^{13}$C, $^{15}$N H2A-H2B |
| | | TRHNCA | 100% $^{2}$H, $^{13}$C, $^{15}$N H2A-H2B |
| | | TRHNCOCA | 100% $^{2}$H, $^{13}$C, $^{15}$N H2A-H2B |
| | Side chain assignments | HBHACONH | 30% $^{2}$H, $^{13}$C, $^{15}$N H2A-H2B; 70% $^{2}$H, $^{13}$C, $^{15}$N H2A-H2B |
| | | HCCCONH | 30% $^{2}$H, $^{13}$C, $^{15}$N H2A-H2B; 70% $^{2}$H, $^{13}$C, $^{15}$N H2A-H2B |
| | | CCCH-TOCSY | 30% $^{2}$H, $^{13}$C, $^{15}$N H2A-H2B; 70% $^{2}$H,$^{13}$C, $^{15}$N H2A-H2B |
| | | $^{15}$N-NOESY-HSQC | 30% $^{2}$H, $^{13}$C, $^{15}$N H2A-H2B; 70% $^{2}$H, $^{13}$C, $^{15}$N H2A-H2B |
| | | $^{13}$C-NOESY-HSQC | 30% $^{2}$H, $^{13}$C, $^{15}$N-H2A-H2B; 70% $^{2}$H, $^{13}$C, $^{15}$N H2A-H2B |
| | NOE identification | $^{15}$N-NOESY-HSQC | $^{13}$C, $^{15}$N H2A-H2B; 30% $^{2}$H, $^{13}$C, $^{15}$N-H2A-H2B |
| | | $^{13}$C-NOESY-HSQC | $^{13}$C, $^{15}$N H2A-H2B; 30% $^{2}$H, $^{13}$C, $^{15}$N H2A-H2B |
| H2A-H2B–RNF169C | Backbone assignments | TRHNCO | 100% $^{2}$H, $^{13}$C, $^{15}$N H2A-H2B–NL RNF169C |
| | | TRHNCOCACB | 100% $^{2}$H, $^{13}$C, $^{15}$N H2A-H2B–NL RNF169C |
| | | TRHNCACB | 100% $^{2}$H, $^{13}$C, $^{15}$N H2A-H2B–NL RNF169C |
| | | TRHNCA | 100% $^{2}$H, $^{13}$C, $^{15}$N H2A-H2B–NL RNF169C |
| | | TRHNCOCA | 100% $^{2}$H, $^{13}$C, $^{15}$N H2A-H2B–NL RNF169C |
| | Side chain assignments | HBHACONH | 30% $^{2}$H, $^{13}$C, $^{15}$N H2A-H2B–NL RNF169C; 70% $^{2}$H, $^{13}$C, $^{15}$N H2A-H2B–NL RNF169C |
| | | HCCCONH | 30% $^{2}$H, $^{13}$C, $^{15}$N H2A-H2B–NL RNF169C; 70% $^{2}$H, $^{13}$C, $^{15}$N H2A-H2B–NL RNF169C |
| | | CCCH-TOCSY | 30% $^{2}$H, $^{13}$C, $^{15}$N H2A-H2B–NL RNF169C; 70%-D, $^{13}$C, $^{15}$N-H2A-H2B–NL RNF169C |
| | | $^{15}$N-NOESY-HSQC | 30% $^{2}$H, $^{13}$C, $^{15}$N H2A-H2B–NL RNF169C |
| | | $^{13}$C-NOESY-HSQC | 30% $^{2}$H, $^{13}$C, $^{15}$N H2A-H2B–NL RNF169C |
| | NOE identification | $^{15}$N-NOESY-HSQC | $^{13}$C, $^{15}$N H2A-H2B–NL RNF169C; 100% $^{2}$H, $^{15}$N H2A-H2B–NL RNF169C |
| | | $^{13}$C-NOESY-HSQC | 30% $^{2}$H, $^{13}$C, $^{15}$N H2A-H2B–NL RNF169C; 70% $^{2}$H, $^{13}$C, $^{15}$N H2A-H2B–NL RNF169C |
| | | $^{13}$C-edited/filtered NOESY | 30% $^{2}$H, $^{13}$C, $^{15}$N H2A-H2B–NL RNF169C; 70% $^{2}$H, $^{13}$C, $^{15}$N H2A-H2B–NL RNF169C |
| | | $^{15}$N-edited/filtered NOESY | 30% $^{2}$H, $^{13}$C, $^{15}$N-H2A-H2B–NL RNF169C; 70% $^{2}$H, $^{13}$C, $^{15}$N H2A-H2B–NL RNF169C |
| | | $^{13}$C-NOESY-aromatic | 30% $^{2}$H, $^{13}$C, $^{15}$N H2A-H2B–NL RNF169C; 70% $^{2}$H, $^{13}$C, $^{15}$N H2A-H2B–NL RNF169C |
| H2A$^{K15ub}$-H2B–RNF169 | Resonance assignments and NOE identification | Methyl-TROSY ($^{13}$C-HMQC) | $^{15}$N, ($^{13}$CH$_3$/$^{12}$CD$_3$-Leu,Val,Ile),$^{12}$C,$^{2}$H H2A-H2B–NL Ub–NL RNF169; $^{15}$N, ($^{13}$CH$_3$/$^{13}$CH$_3$, U-$^{13}$C, $^{2}$H-Leu,Val) $^{12}$C,$^{2}$H H2A-H2B–NL Ub–NL RNF169 |
| | | $^{13}$C-NOESY-HMQC | 30% $^{2}$H, $^{13}$C, $^{15}$N H2A-H2B–NL Ub–NL RNF169C; $^{15}$N, $^{13}$CH$_3$/$^{12}$CD$_3$-Leu,Val,Ile), $^{12}$C,$^{2}$H H2A-H2B–NL Ub–NL RNF169; $^{15}$N, ($^{13}$CH$_3$/$^{12}$CD$_3$-Leu,Val,Ile), $^{12}$C,$^{2}$H H2A-H2B–NL Ub–NL RNF169; $^{15}$N, ($^{13}$CH$_3$/$^{13}$CH$_3$, U-$^{13}$C, $^{2}$H-Leu,Val), $^{12}$C,$^{2}$H H2A-H2B–NL Ub–NL RNF169 |
| | | $^{15}$N-NOESY-HSQC | 30% $^{2}$H, $^{15}$N H2A-H2B–NL Ub–NL RNF169C; $^{15}$N, ($^{13}$CH$_3$/$^{12}$CD$_3$-Leu,Val,Ile), $^{12}$C,$^{2}$H H2A-H2B–NL Ub–NL RNF169; $^{15}$N, ($^{13}$CH$_3$/$^{13}$CH$_3$, U-$^{13}$C, $^{2}$H-Leu,Val), $^{12}$C,$^{2}$H H2A-H2B–NL –NL RNF169 |
| | | $^{13}$C-HSQC | $^{15}$N, ($^{13}$CH$_3$/$^{12}$CD$_3$-Leu,Val,Ile), $^{12}$C,$^{2}$H, H2A-H2B–NL Ub–NL RNF169; $^{15}$N, ($^{13}$CH$_3$/$^{13}$CH$_3$, U-$^{13}$C, $^{2}$H-Leu,Val), $^{12}$C,$^{2}$H H2A-H2B–NL Ub–NL RNF169 |
| RNF169–Ub | Backbone assignments | CBCACONH | $^{13}$C, $^{15}$N RNF169–NL Ub; $^{13}$C, $^{15}$N Ub–NL RNF169 |
| | | HNCACB | $^{13}$C, $^{15}$N RNF169–NL Ub; $^{13}$C, $^{15}$N Ub–NL RNF169 |
| | | HNCO | $^{13}$C, $^{15}$N RNF169–NL Ub; $^{13}$C, $^{15}$N Ub–NL RNF169 |
| | | HN(CA)CO | $^{13}$C, $^{15}$N RNF169–NL Ub; $^{13}$C, $^{15}$N Ub–NL RNF169 |
| | Side chain assignments | HBHACONH | $^{13}$C, $^{15}$N RNF169–NL Ub; $^{13}$C, $^{15}$N Ub–NL RNF169 |
| | | HCCCONH | $^{13}$C, $^{15}$N RNF169–NL Ub; $^{13}$C, $^{15}$N Ub–NL RNF169 |

| | | | |
|---|---|---|---|
| | | CCCH-TOCSY | $^{13}C$, $^{15}N$ RNF169–NL Ub; $^{13}C$, $^{15}N$ Ub–NL RNF169 |
| | NOE identification | $^{15}N$-NOESY-HSQC | $^{13}C$, $^{15}N$ RNF169–NL Ub; $^{13}C$, $^{15}N$ Ub–NL RNF169 |
| | | $^{13}C$-NOESY-HSQC | $^{13}C$, $^{15}N$ RNF169–NL Ub; $^{13}C$, $^{15}N$ Ub–NL RNF169 |
| | | $^{13}C$-edited/filtered NOESY | $^{13}C$, $^{15}N$ RNF169–NL Ub; $^{13}C$, $^{15}N$-Ub–NL RNF169 |
| RNF169N–Ub | Backbone assignments | CBCACONH | $^{13}C$, $^{15}N$ RNF169N–NL Ub; $^{13}C$, $^{15}N$ Ub–NL RNF169N |
| | | HNCACB | $^{13}C$, $^{15}N$ RNF169N–NL Ub; $^{13}C$, $^{15}N$ Ub–NL RNF169N |
| | | HNCO | $^{13}C$, $^{15}N$ RNF169N–NL Ub; $^{13}C$, $^{15}N$ Ub–NL RNF169N |
| | | HN(CA)CO | $^{13}C$, $^{15}N$ RNF169N–NL Ub; $^{13}C$, $^{15}N$ Ub–NL RNF169N |
| | Side chain assignments | HBHACONH | $^{13}C$, $^{15}N$ RNF169N–NL Ub; $^{13}C$, $^{15}N$ Ub–NL RNF169N |
| | | HCCCONH | $^{13}C$, $^{15}N$ RNF169N–NL Ub; $^{13}C$, $^{15}N$ Ub–NL RNF169N |
| | | CCCH-TOCSY | $^{13}C$, $^{15}N$ RNF169N–NL Ub; $^{13}C$, $^{15}N$ Ub–NL RNF169N |
| | NOE identification | $^{15}N$-NOESY-HSQC | $^{13}C$, $^{15}N$ RNF169N–NL Ub; $^{13}C$, $^{15}N$ Ub–NL RNF169N |
| | | $^{13}C$-NOESY-HSQC | $^{13}C$, $^{15}N$ RNF169N–NL Ub; $^{13}C$, $^{15}N$ Ub–NL RNF169N |
| | | $^{13}C$-edited/filtered NOESY | $^{13}C$, $^{15}N$ RNF169N–NL Ub; $^{13}C$, $^{15}N$ Ub–NL RNF169N |
| RNF169N | Backbone assignments | CBCACONH | $^{13}C$, $^{15}N$ RNF169N |
| | | HNCACB | $^{13}C$, $^{15}N$ RNF169N |
| | | HNCO | $^{13}C$, $^{15}N$ RNF169N |
| | | HN(CA)CO | $^{13}C$, $^{15}N$ RNF169N |
| | Side chain assignments | HBHACONH | $^{13}C$, $^{15}N$ RNF169N |
| | | HCCCONH | $^{13}C$, $^{15}N$ RNF169N |
| | | CCCH-TOCSY | $^{13}C$, $^{15}N$ RNF169N |
| | | $^{15}N$-NOESY-HSQC | $^{13}C$, $^{15}N$ RNF169N |
| | | $^{13}C$-NOESY-HSQC | $^{13}C$, $^{15}N$ RNF169N |
| RNF169C* | Backbone assignments | CBCACONH | $^{13}C$, $^{15}N$ RNF169C |
| | | HNCACB | $^{13}C$, $^{15}N$ RNF169C |
| | | HNCO | $^{13}C$, $^{15}N$ RNF169C |
| | | HN(CA)CO | $^{13}C$, $^{15}N$ RNF169C |
| | Side chain assignments | HBHACONH | $^{13}C$, $^{15}N$ RNF169C |
| | | HCCCONH | $^{13}C$, $^{15}N$ RNF169C |
| | | CCCH-TOCSY | $^{13}C$, $^{15}N$ RNF169C |
| Ub | Backbone assignments | CBCACONH | $^{13}C$, $^{15}N$ Ub |
| | | HNCACB | $^{13}C$, $^{15}N$ Ub |
| | | HNCO | $^{13}C$, $^{15}N$ Ub |
| | | HN(CA)CO | $^{13}C$, $^{15}N$ Ub |
| | Side chain assignments | HBHACONH | $^{13}C$, $^{15}N$ Ub |
| | | HCCCONH | $^{13}C$, $^{15}N$ Ub |
| | | CCCH-TOCSY | $^{13}C$, $^{15}N$ Ub |
| | NOE identification | $^{15}N$-NOESY-HSQC | $^{13}C$, $^{15}N$ Ub |
| | | $^{13}C$-NOESY-HSQC | $^{13}C$, $^{15}N$ Ub |

RNF169, RNF169N, RNF169C and RNF169C* are constructs encompassing amino acids 653-708, 653-687, 688-704 and 688-708, respectively. Ub stands for ubiquitin. NL means non-labeled.

**Table S2. NMR and refinement statistics for Ubiquitin–RAD18, Related to Figures 7 and S7**

| | Ubiquitin–RAD18 (198-240) |
|---|---|
| **NMR distance, dihedral and RDC restraints** | |
| Distance restraints | |
| Total nuclear Overhauser effect | 1741 |
| Intra-residue | 434 |
| Inter-residue | 1260 |
| Sequential ($\|i-j\|=1$) | 435 |
| Medium-range ($\|i-j\|\leq 4$) | 277 |
| Long-range ($\|i-j\|\geq 5$) | 548 |
| Intermolecular | 47 |
| Hydrogen bonds | 80 |
| Total dihedral angle restraints | 154 |
| ϕ | 77 |
| ψ | 77 |
| Total RDC restraints | 65 |
| | |
| **Structure statistics** | |
| Violations | |
| Distance restraints (Å) | 0.027 ± 0.008 |
| Dihedral angle restraints (º) | 0.153 ± 0.011 |
| Max. dihedral angle violation (º) | 2.575 ± 0.478 |
| Max. distance violation (Å) | 0.373 ± 0.065 |
| Deviations from idealized geometry | |
| Bond lengths (Å) | 0.005 ± 0.000 |
| Bond angles (º) | 0.580 ± 0.004 |
| Impropers (º) | 0.476 ± 0.012 |
| RDC *Q* | 0.254 ± 0.037 |
| [a]Average r.m.s. deviation to mean structure (Å) | |
| Backbone | 0.34 ± 0.08 |
| Heavy | 0.76 ± 0.06 |
| [a]Average pairwise r.m.s. deviation (Å) | |
| Backbone | 0.49 ± 0.12 |
| Heavy | 1.07 ± 0.13 |
| [a]Ramachandran plot (%) | |
| Most favored regions | 93.8 |
| Additionally allowed regions | 5.8 |
| Generously allowed regions | 0.4 |
| Disallowed regions | 0.0 |

[a]The r.m.s. deviations and Ramachandran plot parameters were calculated for residues ubiquitin (1-71) and RAD18 (201-230) using an ensemble of 20 structures.